J. Marine. Sci. Appl. (2010) 9: 75-80
DOI: 10.1007/s11804-010-8089-x

# Simulating Underwater Plasma Sound Sources to Evaluate Focusing Performance and Analyze Errors

**Tian Ma*, Jian-guo Huang, Kai-zhuo Lei, Jian-feng Chen and Qun-fei Zhang**

*College of Marine Engineering, Northwestern Polytechnical University, Xi'an 710072, China*

**Abstract:** Focused underwater plasma sound sources are being applied in more and more fields. Focusing performance is one of the most important factors determining transmission distance and peak values of the pulsed sound waves. The sound source's components and focusing mechanism were all analyzed. A model was built in 3D Max and wave strength was measured on the simulation platform. Error analysis was fully integrated into the model so that effects on sound focusing performance of processing-errors and installation-errors could be studied. Based on what was practical, ways to limit the errors were proposed. The results of the error analysis should guide the design, machining, placement, debugging and application of underwater plasma sound sources.
**Keywords:** underwater plasma sound source; focusing sound field; error analysis; 3D Max
**Article ID:** 1671-9433(2010)01-0075-06

## 1 Introduction

Underwater plasma sound source (UPSS) is one of the most important applications of underwater pulse discharge technology, in underwater acoustic engineering and seismic survey. It has been used in more and more fields now, such as the deep-sea geological formations detecting (Wang, 2002), acoustic interference source (Pan *et al*., 2008), electro-hydraulic lithotripter (Robin *et al*., 2000), food preservation (Toepfl *et al*., 2007), *etc*. To meet the progressive demand of ultra-long-range underwater communications (ULUC), we either choose the FSK or spread spectrum-modulation which has good performance of noise-resisting and reliability, or increase SNR by increasing sound source-level (SSL). And the former method only can transmit less than 30 km. UPSS, which SSL could reach more than 230 dB (Pan *et al*., 2008), may be used in ULUC more than 100 km in future.

Whatever field UPSS is used in, the components and focusing mechanism of the sound source would be required to study (Zhou and Zhong, 2006). The focusing performance is one of the most important determinant factors of transmitting distance and peak value of the pulse sound wave. And the processing and installing errors would have effect on focusing performance of the sound field. So the error analysis model is required to be built and analyzed.

## 2 UPSS and focusing sound field

### 2.1 Underwater plasma sound source (UPSS)

UPSS is based on the electro-hydraulic effect theory (EHE), proposed by Judkin from the former Soviet Union in 1955. EHE is defined as high voltage and current pulse discharge, going with heat, light and sound, in liquid. Its physical essence is high-speed energy transformation (Wu and Huang, 2003; Qin *et al*., 2000). Fig.1 shows the experiment setup of UPSS.

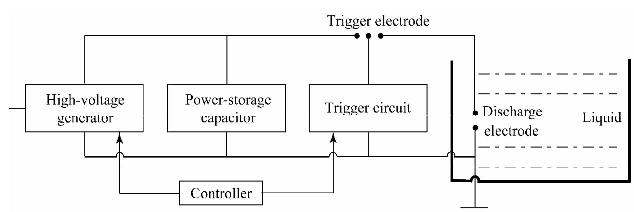


Fig.1 Experiment setup of UPSS

In Fig.1, high-voltage generator, which would raise low voltage to the required high voltage and commute alternating current to direct current, is made up of booster, step-up transformer and rectifier components (Gao *et al*., 2003). The function of power-storage capacitor is to store and discharge the voltage power. When the sound source runs, the controller would control the trigger circuit to generate high-voltage pulse, which would break down and turn on the trigger-electrode. Then the power stored by the capacitor would be added to the two poles of the discharge electrode. When the intensity of the electric field exceeds the critical breakdown intensity, an acute high-voltage discharge would emerge. The discharge process is quite short (μs~ms), but the discharge current is very high (1~100kA). Then a plasma channel would be formed between the two poles of the electrode. Because the channel gains too much energy in quite a short time, its temperature rises quickly and its cubage is heated to expand. Because liquid couldn't be compressed and has inertia, the expanding of the channel would be prevented, and a huge acoustic pulse would emerge, going with ray radiation,

**Received date:** 2008-12-17.
**Foundation item:** Supported by the National Natural Science Foundation under Grant No.60572098.
***Corresponding author Email:** tianxiao888@sina.com

electromagnetic wave and so on. This equipment generating acoustic pulse is called UPSS.

In order to display the micro-process of the underwater plasma electro-acoustics conversion intuitively, a 3-D animation was made by 3DMax's 'Super Spray' tool to simulate the phenomenon of discharge channel formatting and the process of bubble generating, expanding, shrinking and breaking. As shown in Fig.2, firstly, bubbles generate at the two poles of the discharge electrode; secondly, the two expanding bubbles meet and the discharge channel would be formatted; then the discharge bubble would expand and shrink twice (Sun *et al.*, 2005), and break into many small ones finally.

(a) Poles bubble generating

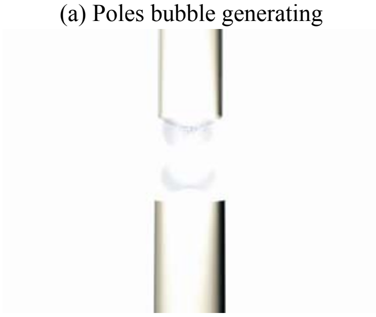

(b) Discharge channel formatting

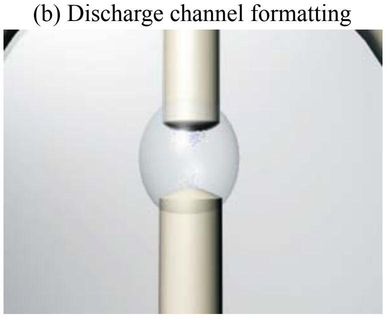

(c) Discharge bubble generating

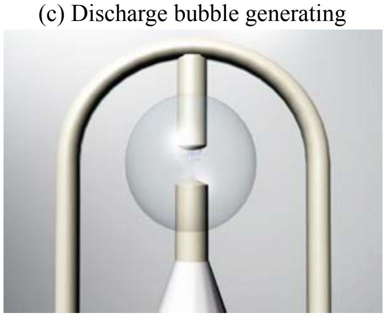

(d) Bubble expanding

(e) Bubble shrinking

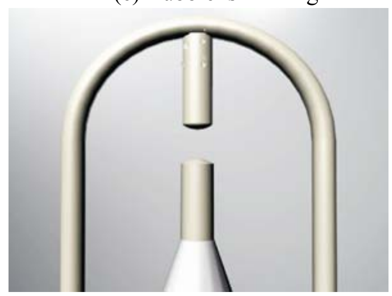

(f) Bubble breaking

Fig.2 The micro-process of the underwater plasma electro-acoustics conversion simulated by 3DMax

The generating ways of UPSS are divided into two kinds (Liu, 2005; Sun *et al.*, 2005). One is spark discharge, which happens only when the distance between the two poles of the electrode is quite short (generally less than 1 cm) and the voltage supplied is high. It has an obvious plasma channel, and could be explained by the prevalent thermal process model. The other is coroner discharge, which happens only when the distance between the two poles of the electrode is longer (generally more than 2 cm) and the voltage supplied is lower, in salt water whose conductance is higher. There isn't a current discharge channel, and only coronary plasma bubbles emerge on the two poles of the electrode. Generally, it could be equivalent to a resistance model. The electric-efficiency of coroner discharge is higher than spark discharge. But coroner discharge is not sensitive to the distance between the two poles of the electrode. Considering that the power of the needed sound source should be alterable and the focusing sound field would be used, spark discharge is chosen to generate this experimental UPSS.

**2.2 Theory of focusing sound field**

Basically, acoustic pulse generated by UPSS is isotropic sphere-wave. If it has not been managed, its intensity would be attenuated rapidly in accordance with the law of square. So its intensity could not achieve the adequate intensity on the appointed direction. In order to increase the launch-efficiency and acoustic intensity in appointed direction, the reflex power-focusing equipment would be required to control the launch direction of the sound source. There are lots of reflex power-focusing equipments, such as acoustic lens, reflective surface (ellipsoid, paraboloid), and so on. According to the practical application, ellipsoid reflector was chosen as the power-focusing equipment. Fig.3 shows the focusing principle of the ellipsoid reflector. As shown in it, *a* is half length of the long-axis, *b* is half length of the short-axis, and *c* is the half focal length. Ellipsoid has two focuses, and acoustic wave, reflected by the reflector, would gather at the second focus ($F_2$), when the sound source is put at the first focus ($F_1$). If make the mouth of the reflector point to the transmitting direction, adequate acoustic intensity would be gained on the appointed direction.

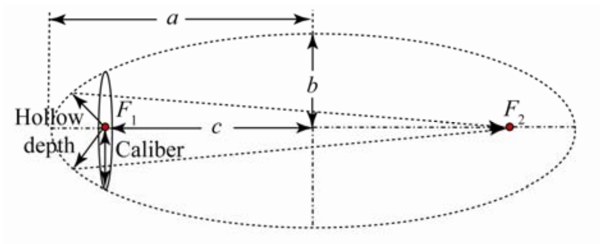


Fig.3 Focusing principle of ellipsoid reflector

### 2.3 Generating of the focusing sound field

According to the principle shown in Fig.1 and Fig.3, an experiment platform was built to generate underwater plasma focusing sound field. The output of high-voltage generator is adjustable (6~10 kV); the power-storage capacitor is composed of four parallel-connected high-voltage pulse capacitors (0.2 μF/15 kV), and its total capacitance is 0.8 μF. The field-distortion switch, triggered by high-voltage, was used to control the trigger-electrode. The distance between the two poles of the discharge-electrode, which is made of copper-alloy and adopts the tine-tine structure, is 2 mm. The water container is made of Plexiglas-cylinder, whose diameter is 20 mm and height is 80 mm. The reflector, whose inner surface is ellipsoid, is made of stainless steel and its focus is 80 mm.

Fig.4 shows the typical pressure wave, measured at the second focus ($F_2$, 160 mm away from the sound source) by piezoelectric pressure sensors 138A06.

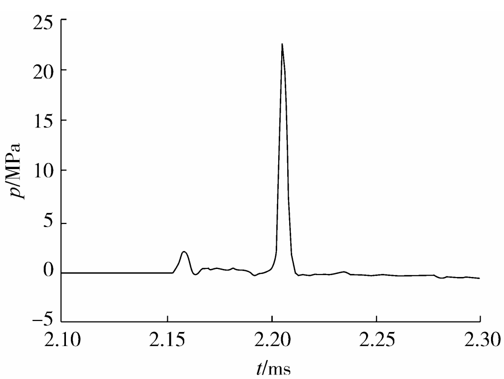


Fig.4 Typical pressure wave at the second focus ($F_2$)

As shown in Fig.4, there are two main pulses, the former is direct wave and the latter is focused wave, and their peak pressure (*p*) ratio is about 1:10. The acoustic pressure of the focused wave is 22.54 MPa, which is about 0.58 MPa converted acoustic pressure 1 m away from the sound source, so its SSL is about 235 dB. This shows that UPSS has high instant acoustic launch-power, narrow pulse and great peak energy. If the reflective technology is applied, the high-directional beam pulse would be formed. So UPSS may be used in ULUC in future.

## 3 Focusing performance of the sound field and error analysis

Because there are inevitable errors in the processing of the reflector, its hollow-depth and caliber would have a bias. This, called processing error, might cause the position of the first focus to move away. When the discharge-electrode is fixed, it would bias from the first focus. This is called installation error. All these errors may have effect on the distributing and focusing performance of the sound field. So the effects, caused by processing error and installation error, require an in-depth study for the purpose of practical applications.

Software ANSYS (Howard *et al*., 2005) is quite suitable for simulating the dynamic transmit-distributing of the focusing sound field. This job was done by the other researcher in the group. Fig.5 shows the four acoustic-distributing stages of the focusing sound field, simulated by ANSYS. And the first figure shows the initial stage of the discharging progress; in the second figure, the sounds spread down just meet the reflector; in the third figure, the reflected sounds are focused at $F_2$; in the forth figure, the focused sounds is fading away in the end.

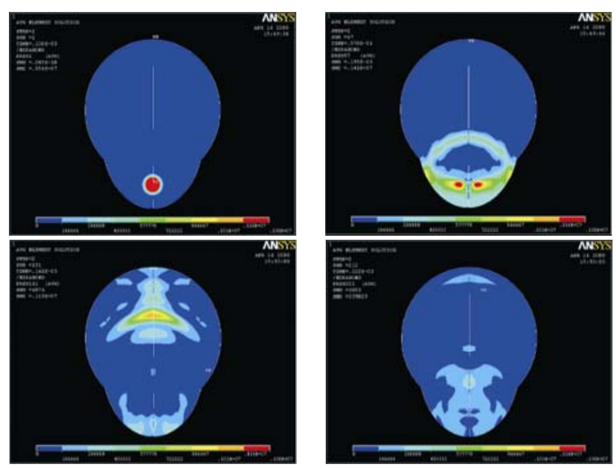

Fig.5 Acoustic-distributing simulated by ANSYS

According to the practical applications, ANSYS was not quite suitable for quantitative analyses of these errors, so the software 3D Max was chosen to do these jobs. The detailed steps are as follows:

As shown in Fig.6, a custom complex particle-system was established to simulate the acoustic wave, by ‘particle view’ tool (Wang, 2006). The shape of the reflector was established by the ‘ellipse’ and ‘turning’ tools, and its function was simulated by ‘collision-detection’ and ‘full-director’ tools. Table

1 shows the setting of the parameters. After the system has been set up, the position of the sound source could be moved easily, and the shape of the reflector also could be changed expediently. The moving path of the sound wave could be calculated automatically by 3D Max. Then the still focusing situation could be observed expediently, by dragging the frame to the position that the waves gathered. As the analyzed structure is axisymmetric, the error analysis, based on the 3-D space, could be simplified to 2-D. Thus, the analysis complexity would be reduced, and the result would be more intuitive.

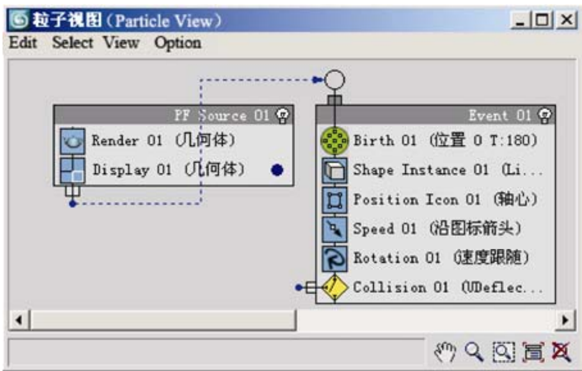


Fig.6 Custom complex particle-system

As shown in Fig.7, the simulation model had been established according to Table 1, and the focusing situation without any error is consistent with the theoretical analysis. There are 128 lines gathered at $F_2$.

**Table 1 Main parameter setting in 3D Max**

| *a*/mm | *b*/mm | *c*/mm | Amount |
|---|---|---|---|
| 120 | 90 | 80 | 200 |
| Speed/(m·s$^{-1}$) | Shape | Icon | Radiation |
| 100 | 'Line 1' | 'axes' | 180 |
| Start/Stop | Deflector | Speed | |
| 0 | 'UDef 1' | 'rebound' | |

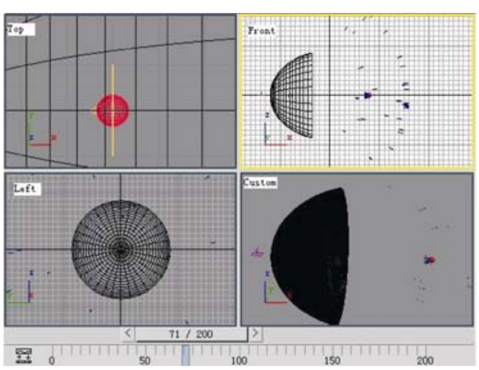


Fig.7 Simulation mode of focusing performance

### 3.1 Processing error analysis

In the processing, hollow-depth of the reflector would be rare generally, so the caliber error is the main processing-error. As shown in Figs.8~10, it is the same that, every small pane is 10mm×10mm, and the left red-point is at the position of $F_1$ (-80 mm, 0) and the right $F_2$ (80 mm, 0). Fig.8(a) shows the focusing performance affected by caliber error, which is 2mm longer than the standard and Fig.8(b) 5 mm longer, and Fig.8(c) 2 mm shorter, and Fig.8(d) 5 mm shorter. Seen from the figure, caliber error doesn't have too much effect on the focusing position ($F_2$) and the number of focused lines. But the interval becomes longer and longer with the error increase. This makes the focused energy dispersed along the length of time and the peak value of the focusing point reduced.

### 3.2 Installation error analysis

The installation error could be simplified into the errors along *x*-axis and *y*-axis.

Fig.9 shows the focusing performance affected by the installation position bias from $F_1$ along *x*-axis. As shown in the first figure, when the installation position was (-78 mm, 0), which was +2 mm biased from $F_1$ along *x*-axis, the focusing position would be (70.5 mm, 0), 9.5 mm in front of $F_2$ and there were 124 lines gathered; in the second figure, when the installation position was (-75 mm, 0), which was +5 mm biased from $F_1$ along *x*-axis, the focusing position would be (57.5 mm, 0), 22.5 mm in front of $F_2$ and there were 125 lines gathered; in the third figure, when the installation position was (-82 mm, 0), which was -2 mm biased from $F_1$ along *x*-axis, the focusing position would be (98.5 mm, 0), 18.5 mm behind $F_2$ and there were 128 lines gathered; in the forth figure, when the installation position was (-85 mm, 0), which was -5 mm biased from $F_1$ along *x*-axis, the acoustic line would not gather yet, but the densest position was (-44.5 mm, 0).

Seen from the first two figures in Fig.9, the focusing position would bias from $F_2$ along the negative position of *x*-axis, when the installation position biased from $F_1$ along the positive position of *x*-axis. Although the number of the focused lines was almost the same, the focused energy dispersed along the width. This made the focus-spot become bigger. Seen from the last two figures, the focusing position would bias from $F_2$ along the positive position of *x*-axis, when the installation position biased from $F_1$ along the negative position of *x*-axis. The number of the focused lines was also almost the same, but when the bias was bigger than 4 mm, the acoustic line would not gather yet and would spread forward in parallel, then disperse.

Fig.10 shows the focusing performance affected by the installation position biased from $F_1$ along the positive position of *y*-axis. As shown in the first figure, when the installation position was (-80 mm, 2 mm), which was +2 mm biased from $F_1$ along *y*-axis, the focusing position would be (80 mm, -6.5mm), 6.5 mm down from $F_2$ and there were 128 lines gathered; in the second figure, when the installation position was (-80 mm, 5 mm), which was +5 mm biased from $F_1$ along *y*-axis, the focusing position would be (80 mm, -17.5mm), 17.5 mm down from $F_2$ and there were 126 lines gathered. Seen from the two figures, the focusing position would bias from $F_2$ along the negative position of *y*-axis, when the installation position biased from $F_1$ along the positive position of $y$-axis. Although the number of the focused lines was almost the same, the focused energy dispersed along the width. This made the focus-spot become bigger. As this system is symmetric about $x$-axis, the focusing performance affected by the installation position biased from $F_1$ along the negative position of $y$-axis is similar, and would be omitted here.

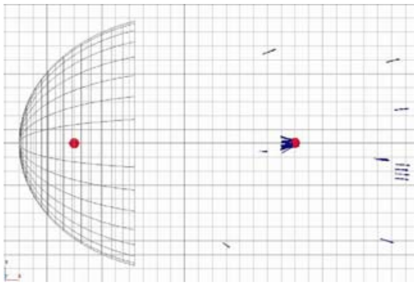

(a) caliber+2 mm

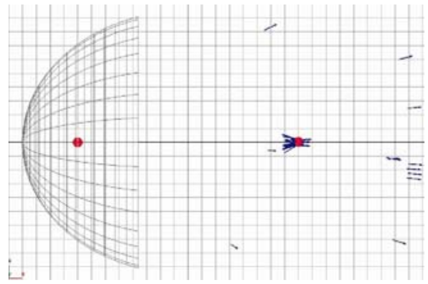

(b) caliber+5 mm

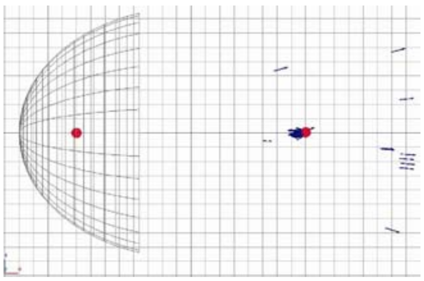

(c) caliber-2 mm

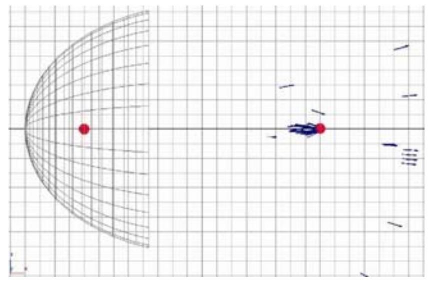

(d) caliber-5 mm

Fig.8 Front view of focusing performance affected by caliber error

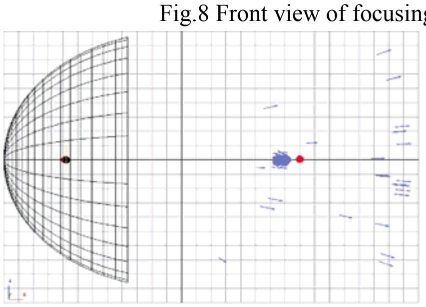

(a) $x$-axis bias+2 mm

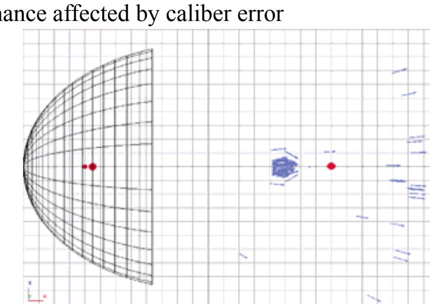

(b) $x$-axis bias+5 mm

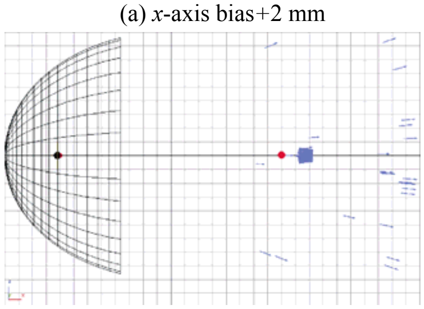

(c) $x$-axis bias-2 mm

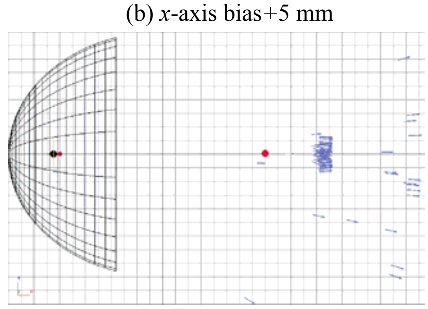

(d) $x$-axis bias-5 mm

Fig.9 Front view of focusing performance affected by the installation position bias from $F_1$ along $x$-axis

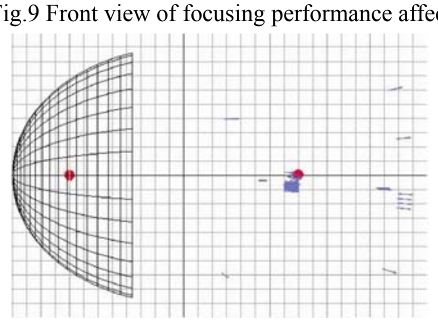

(a) $y$-axis bias+2 mm

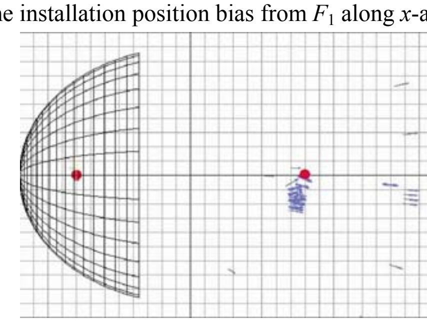

(b) $y$-axis bias+5 mm

Fig.10 Front view of focusing performance affected by the installation position biased from $F_1$ along $y$-axis

# 4 Conclusions

1) The components and focusing mechanism of the sound source were analyzed. If the reflective technology is applied, the acoustic wave, generated by UPSS, may have high instant acoustic launch-power, narrow pulse, high peak energy and great directivity.

2) Processing-error of caliber doesn't have too much effect on the focusing position ($F_2$) and the number of focused lines. But the focused energy would disperse with the time passing and the peak value of the focusing point would be reduced.

3) Little installation-error would have bigger effect on the focusing position ($F_2$) and energy. In order to achieve the adequate focusing performance, installation-error needs to be strictly restricted.

4) When the bias of the focusing position is limited to less than 1 mm, the processing-error needs to be less than 1 mm; and the installation-error along the positive position of $x$-axis needs to be less than 0.2 mm, along the negative position less than 0.16 mm; and the installation-error along $y$-axis needs to be less than 0.3 mm.

# References

Gao Bo, Zhang Hanhong, Zhang Chi (2003). Experimental investigation of bublles by underwater wire exploding. *Acta Physica Sinic*, **52**(7), 1714-1719. (in Chinese)

Howard CQ, Hansen CH, Zander AC (2005). Multi-variable optimization of a vibro-acoustic system using a distributed computing network. *Twelfth International Congress on Sound and Vibration*, Lisbon, 1-7.

Liu Qiang (2005). *The study of pulsed corona discharge in water*. Chinese Academy of Sciences, Beijing, 25-28. (in Chinese)

Pan Xiaojing, Huang Jianguo, Chen Jun (2008). Study on underwater wideband acoustic interference source based on electro-hydraulic effect. *Audio Engineering*, **32**(5), 66-68. (in Chinese)

Qin ZY, Zuo GN, Wang YR (2000). *Strong high-voltage pulse discharge and its application*. Beijing Industrial University Press, Beijing, 6-16. (in Chinese)

Robin OC, Bailey MR, Fineberg N, Hartenbaum B, Lokhandwalla M, McAteer JA, Sturtevant B (2000). Design and characterization of a research electro-hydraulic lithotripter patterned after the Dornier HM3. *Review of Scientific Instruments*, **71**(6), 2514-2525.

Sun Yaohong, Zhou Yuanxiang, Jin Mingjian, Liu Qiang, Yan Ping (2005). New prototype of underwater sound source based on the pulsed corona discharge. *Journal of Electrostatics*, **63**(6-10), 969-975.

Toepfl S, Heinz V, Knorr D (2007). High intensity pulsed electric fields applied for food preservation. *Chemical Engineering and Processing*, **46**, 537-546.

Wang Runtian (2002). Progress in detecting the geological formations and sediment properties by sound. *Technical Acoustics*, **21**(1-2), 96-98. (in Chinese)

Wang Xiaoguang (2006). *3ds max video effects performance techniques*. Weapon Industry Press and Beijing Hope Electronic Press, Beijing, 232-256. (in Chinese)

Wu Weimin, Huang Suangxi (2003). Application and development of high power pulse discharge under water. *Modern Electronic Technology*, (5), 85-89. (in Chinese)

Zhou Yufeng, Zhong Pei (2006). The effect of reflector geometry on the acoustic field and bubble dynamics produced by an electrohydraulic shock wave lithotripter. *The Journal of the Acoustical Society of America*, **119**(6), 3625-3636.

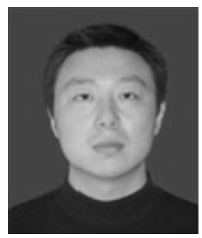

**Tian Ma** was born in 1982. He is a PhD candidate at the College of Marine, Northwestern Polytechnical University. His current research interests include underwater acoustic simulation, virtual reality technology and multimedia, *etc*.

**Jian-guo Huang** was born in 1945. He is a professor and a doctoral advisor in signal processing and underwater acoustic at NWPU. He is a fellow of Chinese Society of Acoustics, Senior Member of IEEE, and Chairman of IEEE in Xi'an section of China.

**Kai-zhuo Lei** was born in 1965. He is an associate professor at NWPU. His current research interests include underwater acoustic engineering, electrical source technology, *etc*.